

# Functional Consequence of Mutating Conserved Residues of the Yeast Farnesyl-Protein Transferase $\beta$ -Subunit Ram1(Dpr1)<sup>†</sup>

David D. Kurth, Lynn Farh, and Robert J. Deschenes\*

Department of Biochemistry, University of Iowa, Iowa City, Iowa 52242

Received July 3, 1997; Revised Manuscript Received October 17, 1997<sup>®</sup>

**ABSTRACT:** Ras proteins, fungal mating pheromones, and other proteins terminating in the sequence CaaX (where C is Cys, a is any aliphatic amino acid, and X is the C-terminal residue) are posttranslationally prenylated. Farnesyl-protein transferase (FPTase) transfers the farnesyl moiety of farnesyl pyrophosphate (FPP) to the thiol of the CaaX box cysteine in a reaction that requires  $\text{Zn}^{2+}$  and  $\text{Mg}^{2+}$ . We have created mutations in conserved amino acids of the yeast Ram1 protein to identify residues important for  $\text{Zn}^{2+}$ -dependent FPTase activity. Wild-type and mutant Ram1 proteins were expressed as operon fusions in bacteria, and FPTase activity was measured. Mutations in conserved residues Glu256, His258, Asp307, Cys309, Asp360, and His363 reduce FPTase activity. Asp307, Cys309, and His363 correspond to the residues that have been shown to coordinate  $\text{Zn}^{2+}$  in mammalian FPTase. The H258N mutant enzyme exhibited an increased sensitivity to the  $\text{Zn}^{2+}$  chelator 1,10-phenanthroline, required higher concentrations of  $\text{Zn}^{2+}$  to restore activity to the apoenzyme, and had a 10-fold reduction in catalytic efficiency. The decreases in FPTase activity observed do not appear to be caused by major structural perturbations because the mutants were stably expressed and retained the ability to interact with Ram2p during purification. The FPTase activity of the mutants measured *in vitro* correlated well with their ability to complement the mating and growth defects of a *ram1Δ* strain *in vivo*.

Ras proteins, fungal mating pheromones, and a growing list of proteins terminating in the sequence CaaX (where C is Cys, a is any aliphatic amino acid, and X is the C-terminal residue)<sup>1</sup> are posttranslationally modified by prenylation of the CaaX box cysteine, proteolytic removal of the –aaX residues, and carboxyl methylation (1–4). Many prenylated proteins are also palmitoylated on a second cysteine upstream of the CaaX box (3–5). Three prenyl-protein transferases have been described. Proteins terminating in a CaaX box in which the X residue is Ser, Met, Cys, or Ala are farnesylated by the enzyme farnesyl-protein transferase (FPTase) (6–8), whereas if X is Leu, the protein is geranylgeranylated by a type I geranylgeranyl-protein transferase (GGPTaseI) (7, 9–11). Although FPTase and GGPTaseI have the highest affinity toward CaaX boxes terminating in these “X” residues, they are able to utilize other CaaX box sequences both *in vitro* and *in vivo* (12, 13). The third prenyltransferase, GGPTaseII, geranylgeranylates proteins such as rab proteins that terminate in the sequence –CC or –CXC (7, 14, 15).

FPTases have been isolated and characterized from a variety of animal and plant sources (4). In yeast, the enzyme is a heterodimer composed of a conserved  $\alpha$  subunit (37 kDa) encoded by *RAM2* and a  $\beta$  subunit (43 kDa) encoded by *RAM1(DPR1)* (16–21). A common  $\alpha$  subunit (Ram2p) is

shared between GGPTaseI and FPTase. Distinct  $\beta$  subunits account for the difference in specificity observed between the two prenyltransferases (10, 22, 23). Detailed kinetic analysis has been performed on purified bovine, human, and yeast FPTase enzymes (24–27). Although formally a random sequential mechanism, the preferred mechanism appears to be ordered with the prenyl substrate adding first (25–27). Product release is the rate-limiting step in catalysis, and the product release is triggered by the addition of substrate (28, 29).

FPTase is a metalloenzyme that requires  $\text{Zn}^{2+}$  and  $\text{Mg}^{2+}$ . In mammalian FPTases, CaaX substrate binding requires  $\text{Zn}^{2+}$ , whereas the prenyl substrate binds in the absence of  $\text{Zn}^{2+}$  (30, 31).  $\text{Zn}^{2+}$  is believed to play a direct role in catalysis by coordinating the CaaX thiol in the enzyme–FPP–peptide substrate ternary complex (32). Asp297, Cys299, and His362 of the mammalian FPTase  $\beta$  subunit have been shown to coordinate  $\text{Zn}^{2+}$  in mammalian FPTase. The corresponding residues are conserved in the yeast  $\beta$  subunit, Ram1. We have mutated these residues and other conserved His and Cys residues, expressed the mutant enzymes in bacteria, and measured their enzymatic properties. The results obtained with yeast FPTase have been interpreted with the help of the recently reported 2.25-Å crystal structure of the mammalian FPTase (33).

## EXPERIMENTAL PROCEDURES

**Materials.** Unless otherwise stated, all restriction enzymes, T4 DNA ligase, and other DNA-modifying enzymes were purchased from New England Biolabs and used according to the manufacturers' instructions. *In vitro* mutagenesis was done using an oligonucleotide-directed *in vitro* mutagenesis system (Amersham). [ $1\text{-}^3\text{H}$ ]Farnesyl py-

<sup>†</sup> This work was supported in part by a grant from the National Institutes of Health (CA50211) to R.J.D.

\* Address correspondence to this author. Telephone: 319-335-7884. FAX: 319-335-9570. E-mail: robert-deschenes@uiowa.edu.

<sup>®</sup> Abstract published in *Advance ACS Abstracts*, December 1, 1997.

<sup>1</sup> Abbreviations: FPTase, farnesyl-protein transferase; GGPTase, geranylgeranyl-protein transferase; FPP, farnesyl pyrophosphate; CaaX, C is Cys, a indicates aliphatic amino acid, and X is any amino acid; ECL, enhanced chemiluminescence; SDS–PAGE, sodium dodecyl sulfate–polyacrylamide gel electrophoresis; PCR, polymerase chain reaction; PMSF, phenylmethanesulfonyl fluoride; kDa, kilodalton.

Table 1: Mutagenic Primers Used in Preparation of *RAM1* Mutants

mutant	primer <sup>a</sup>
H83N	3'-GCTTTCTCAAACCTGTTTACATG-5'
H156Q	3'-GGTTAATAGAGTTAACCGTTCG-5'
H253N	3'-CCGTCAACAGGATTGCATCTACTCC-5'
E256Q <sup>b</sup>	3'-GGAGTGCATCTA(C/G)TCCGT(G/T)TGCCTCCGATATG-5'
H258N <sup>b</sup>	
D307N	5'-GCAACAAACTTGTTAATGGTTGCTATAGTTTTTG-5'
C309A	5'-CAACAAACTTGTTGATGGTGCCTATAGTTTTGGGT-5'
H363Q	3'-CTGAAAATGGTTTGTAAATAACG-5'
C367A	5'-TACCATACAAATTATGCATTATTAGGACTGGCTGTT-3'

<sup>a</sup> Mutant anticodon underlined. <sup>b</sup> E256Q and H258N are generated by the same degenerate oligonucleotide

rophosphate (15 Ci/mmol) was purchased from American Radiolabeled Chemicals Inc. The NTA-Ni resin used to purify His-tagged proteins was obtained from Qiagen. Western blots were visualized by enhanced chemiluminescence (ECL) (Amersham). Film for fluorography was purchased from Kodak. All yeast media and agar were purchased from Difco and prepared according to standard procedure (34). All other reagents were purchased from Mallinckrodt or EM Science.

**Strains and Plasmid Constructions.** The pUC119-Ram1 and pBC-KS(+)-6xHis-Ram2 plasmids were kindly provided by Drs. Scott Powers and Mark Marshall, respectively. Details of their construction can be found elsewhere (8, 35). To construct the myc epitope-tagged Ram1 expression plasmid, the strain TG1 harboring pUC119-Ram1 was infected with the M13K07 helper phage to produce a single-stranded template of pUC119-Ram1. The myc epitope was cloned upstream and in-frame with the 5' end of the *RAM1* open reading frame by oligonucleotide-directed mutagenesis (Amersham). The sequence of the oligonucleotide (non-coding strand) that introduced the nine-amino acid tag was 5'-CCTACTCTCTGTCGCATCAAGTCTTCTTCAGAAATAAGCTTTTGTTCATGGTCATAGCTGTTTCC-3'. The resulting plasmid, pUC119-(myc)-Ram1, was used to construct the Ram1 mutants described in this paper. The oligonucleotides used to create the mutations are listed in Table 1.

A *RAM2/RAM1* operon fusion plasmid (pRJ493) was used to overexpress yeast FPTase. It was constructed as follows. A 6xHis-T7 epitope-tagged *RAM2* plasmid (pRJ499) was obtained by polymerase chain reaction (PCR) amplification using pBC-KS(+)-6xHis-Ram2 as a template, *XhoI*-T7 primer at the 3' end of *RAM2* (5'-CCGCTCGAGTAATACGACTCACTATAG), and a T3 promoter primer upstream of *RAM2* (5'-ATTAACCCTCACTAAAGGGA). The PCR fragment was digested with *XhoI* and ligated into the *XhoI* site of pET28c (Novagen). Myc epitope-tagged *RAM1* was generated by PCR using primers to the 5' and (5'-GGGAATTCATATGGAACAAAAGCTTATTTCTGA-3') and 3' end (5'-CGCGGATCCGTAAAACGACGGCCAGTGAAT-3') of pUC119-(myc)*RAM1*. The fragment was digested with *NdeI* and *BamHI* and ligated into pET11a (Novagen) digested with *NdeI* and *BamHI*. The (6xHis-T7)*RAM2* fragments were excised from pRJ499 with *XbaI* and inserted it into the *XbaI* site of pET11a-myc-*RAM1*(B487). The resulting operon fusion plasmid, pRJ493, was transformed into BL21(DE3) bacterial cells for expression and purification.

The plasmids for *in vivo* studies were constructed by homologous recombination beginning with pSB32Ram1. The plasmid pSB32 was made by replacing the *URA3* gene of

YCP50 (36) with *LEU2* (Joshua Trueheart, unpublished results). The *RAM1* gene carried on pSB32 was digested with *NcoI*, and a *XbaI* linker was inserted destroying the *NcoI* site. The mutant *RAM1* gene fragments were generated by PCR amplification primers to the 5' and (5'-ATGCGACAGAGAGTAGGAAGGT-3') and 3' end (5'-GACTGACCGCTAAGGAGATTGA-3') of Ram1 cloned in pUC119. The PCR-generated fragments were transformed, along with pSB32Ram1, and gapped with *XbaI*, into the yeast strain RJY266 (37) using the method of Ito et al. (38). The resulting transformants were selected by their ability to grow on synthetic medium plates lacking leucine (SC-Leu, 2% glucose). Plasmids were rescued from the leucine prototrophs (39) and used to transform *Escherichia coli* strain MC1066. Plasmid DNA was purified and screened for the presence of the *NcoI* restriction site. The presence of the mutation was confirmed by sequence analysis.

**Expression and Purification of Bacterially Expressed Yeast FPTase.** Cultures of BL21(DE3) harboring the *RAM2/RAM1* operon fusion plasmid were grown to midlogarithmic phase ( $A_{600} = 0.700$ ) and induced with 1 mM IPTG for 2 h. Cells were pelleted at 4000g for 30 min, washed once with extraction buffer (50 mM Tris-Cl, pH 7.4, 0.1 mM MgCl<sub>2</sub>, 0.1 mM EGTA, 2 mM PMSF, and 5% glycerol), and again pelleted at 4000g for 30 min. The cells were lysed with a French press in extraction buffer containing 2 mM PMSF and fractionated by centrifugation for 1 h at 50000g in a Beckman SW41Ti swinging bucket rotor. The soluble extracts (*S*<sub>50</sub>) were aliquoted, frozen on dry ice, and stored at -80 °C.

Nickel affinity chromatography (Ni-NTA, Qiagen) was used to purify FPTase. Approximately 32 mg of the soluble protein extract in 10 mL of Ni-NTA binding buffer (50 mM Tris, pH 8, 100 mM NaCl, 0.1% Tween-20) was mixed with 1 mL of Ni-NTA resin (50% in Ni-NTA binding buffer), and the mixture was incubated at 4 °C for 1 h. The resin was collected by centrifugation (1000g, 1 min) and washed three times with 8 mL of Ni-NTA binding buffer containing protease inhibitors (1 µg/mL chymostatin, 1 µg/mL pepstatin A, and 0.02 mg/mL aprotinin), four times with 8 mL of Ni-NTA binding buffer containing 10 mM imidazole, once with 1 mL of Ni-NTA containing 60 mM imidazole, and finally once with 1 mL of 10 mM β-mercaptoethanol in thrombin cleavage buffer (50 mM Tris, pH 8, 150 mM NaCl, 2.5 mM CaCl<sub>2</sub>). FPTase was eluted by incubating for 10 min in 1 mL of thrombin cleavage buffer containing 3 units/mL thrombin (Sigma). Glycerol was added to a final concentration of 10%, and the samples were stored at -80 °C. More highly purified enzyme for kinetic analysis was obtained using FPLC equipped with a MonoQ column equilibrated

with 50 mM NaCl in MonoQ buffer (50 mM Tris, pH 7.5, 1 mM DTT, and 20  $\mu$ M ZnCl<sub>2</sub>). Purified FPTase was found to elute at approximately 250 mM NaCl. Glycerol was added to each sample to obtain a final concentration of 20%, and samples were stored at  $-80^{\circ}\text{C}$ .

**FPTase Activity Assays.** A qualitative gel assay of FPTase activity was performed using Ras1T(CIIS) protein as a substrate. Ras1T(CIIS) was provided by Dr. Mark Marshall (Indiana University) and was constructed by deleting the hypervariable domain and changing the CaaX box of yeast Ras1 to produce a 25-kDa protein terminating in the CaaX box, CIIS. A typical FPTase reaction included 2  $\mu$ M Ras1T(CIIS), 0.1  $\mu$ Ci [<sup>3</sup>H]farnesyl pyrophosphate (15 Ci/mmol), and 1  $\mu$ g of S<sub>50</sub> protein in a reaction volume of 20  $\mu$ L. The reaction buffer was 20 mM Tris-Cl, pH 7.4, 100 mM NaCl, 5 mM MgCl<sub>2</sub>, 20  $\mu$ M ZnCl<sub>2</sub>. The reaction was incubated at 25  $^{\circ}\text{C}$  for 10 min, stopped by addition of 5  $\mu$ L of 5 $\times$  concentrated SDS-PAGE loading buffer, heated at 95  $^{\circ}\text{C}$  for 3 min, and resolved by SDS-PAGE (12.5% gel). Fluorography was performed following FluoroEnhance treatment (Research Products International).

A fluorescence FPTase assay using a dansyl-GCIIS peptide was performed essentially as described (40, 41). The reaction mixture (120  $\mu$ L) consisted of 50 mM Tris, pH 7.4, 12 mM MgCl<sub>2</sub>, 12  $\mu$ M ZnCl<sub>2</sub>, 5.8 mM DTT, 0.04% dodecyl  $\beta$ -maltoide, 0.5–2.4  $\mu$ M dansyl-GCIIS, and 0.4–7  $\mu$ M FPP. Prior to the initiation of the reaction the assay components were incubated for 5 min at 30  $^{\circ}\text{C}$ . To initiate the reaction, 52 ng of wild-type or 238 ng of mutant FPTase was added to the reaction mixture in a 3-mm quartz cuvette. Fluorescence enhancement ( $\lambda_{\text{ex}} = 340$  nm;  $\lambda_{\text{em}} = 500$  nm) was monitored using a SLM 4800 fluorometer. A 300-s progress curve was recorded and the initial velocity determined from the slope using a parabolic least-squares curve-fit method. The apparent  $K_m$ 's were estimated by fitting the data with the Cleland's Kinetics program assuming Michaelis–Menton kinetics.

**[<sup>3</sup>H]Farnesyl Pyrophosphate Binding to Reconstituted Yeast FPTase.** FPP binding was performed as described (30) using 6xHis-tagged yeast FPTase purified by the Ni affinity column. Briefly, FPTase was incubated with 100 pmol of [<sup>3</sup>H]FPP (2200 dpm/pmol) in 20  $\mu$ L of binding buffer (20 mM Tris-Cl, pH 7.4, 100 mM NaCl, 5 mM MgCl<sub>2</sub>, 20  $\mu$ M ZnCl<sub>2</sub>) at 25 $^{\circ}\text{C}$  for 15 min. Bound [<sup>3</sup>H]FPP was separated from free label using a Sepharose G50 gel filtration column (0.7 cm  $\times$  4.5 cm). Fractions (80  $\mu$ L) were collected, and the radioactivity was measured by scintillation counting. To assess the effect of Zn<sup>2+</sup> on FPP binding, the Ni column-purified FPTase was first dialyzed in Zn<sup>2+</sup>-free buffer (see above) or chelated with 1 mM 1,10-phenanthroline to remove endogenous Zn<sup>2+</sup>, and the column was equilibrated with Zn<sup>2+</sup>-free binding buffer (20 mM Tris-Cl, pH 7.4, 100 mM NaCl, 5 mM MgCl<sub>2</sub>).

**Activity of Ram1 Mutants in Vivo.** A MATa haploid RAM1 null mutant was obtained by sporulating heterozygous diploid strain, SM1590, obtained from Dr. Susan Michaelis (Johns Hopkins) (MATa/ $\alpha$  leu2-3,112/leu2-3,112 ura3-52/ura3-52 his4/his4 RAM1/ram1::URA3). The resulting haploid, RJY871 (MATa ram1::URA3 leu2-3,112 his4), was then transformed with either pSB32Ram1 or pSB32 plasmids expressing mutant RAM1 genes [Ram1(H258N), Ram1(E256Q), Ram1-(E256Q/H258N), or Ram1(H253N/H258N)]. A homologous recombination strategy (42) was used to construct the

plasmids expressing the mutants. In the first step, the coding regions of the mutant RAM1 genes are amplified by PCR. In the second step, the fragment is mixed with pSB32Ram1 that had been gapped with restriction enzymes. Recombination between the two fragments occurs upon transformation of strain RJY871 with PCR fragment and the gapped plasmid. The sequence of the Ram1 insert was confirmed by sequence analysis. Quantitative mating assays were performed by mixing  $7 \times 10^6$  cells of strain RJY871 ( $2 \times 10^7$  cells/mL) harboring wild-type or mutant constructs of Ram1 with  $3.5 \times 10^7$  cells of a midlog culture of strain RJY102 (MATa leu2-3,112 ura3-52 his3). The mixture was spun briefly (1 min, 2000 rpm) to form a loose pellet of cells, and the mating reaction was allowed to proceed for 6 h at room temperature. The cells were diluted with synthetic medium lacking leucine (SC-Leu, 2% glucose) and plated on either SC-Leu or SC-His (only diploids grow). The mating efficiency was determined by dividing the number of colonies that grow on SC-His plates by the number of colonies that grow on the SC-Leu plate.

**Determination of the Growth Rate.** A fresh overnight culture of RJY871 expressing wild-type or mutant Ram1 alleles was diluted into YEPD medium to a final concentration of  $1 \times 10^6$  cells/mL and incubated at 30  $^{\circ}\text{C}$  with agitation. At 2-h intervals, 200  $\mu$ L was removed and placed in a 96-well flat-bottom microtiter plate, and the optical absorbance was measured (Abs<sub>660</sub>) using Titertek Multiskan MCC/340.

## RESULTS

**Expression of Yeast FPTase Subunits in Bacteria and Reconstitution of Activity.** Previous studies have shown that production of functional FPTase requires coexpression of the  $\alpha$ - and  $\beta$ -subunit genes, presumably because the two subunits are unstable unless association occurs during, or shortly after, synthesis (8, 43, 44). We began by examining whether the yeast FPTase subunits behaved similarly. The RAM1 gene ( $\beta$  subunit) was expressed as an in-frame fusion with an amino-terminal myc epitope tag (H<sub>2</sub>N-MTMEQKLISEEDL-Ram1). The RAM2 gene ( $\alpha$  subunit) was expressed with a 6xHis tag at its amino terminus. FPTase activity was measured following coexpression of RAM1 and RAM2 in one strain or after reconstituting the enzyme from extracts of two strains expressing each subunit independently. No difference in activity was observed (Figure 1, panel A). Immunoblot analysis revealed that similar levels of Ram1p were produced whether the RAM1 gene was expressed alone or in combination with RAM2 (Figure 1, panel B).

**Mutations in Conserved Residues of Ram1 Affect FPTase Activity.** The amino acid sequences of the three cloned FPTase  $\beta$ -subunit genes and the yeast GGPTase  $\beta$  subunit, Cal1, were aligned, and five conserved blocks of sequence containing conserved histidine, cysteine, and acidic residues were identified (Figure 2). We changed each of these residues either alone or in combination as indicated in Table 1. Asp307, Cys309, and His363 correspond to residues that have been shown to coordinate Zn<sup>2+</sup> in mammalian FPTase crystal structure (33). The mutations created do not appear to grossly perturb the structure of Ram1 or its ability to interact with Ram2p. This was shown by mixing extracts from bacteria expressing wild-type or mutant Ram1p with (6xHis)Ram2p and measuring the ability of the two subunits

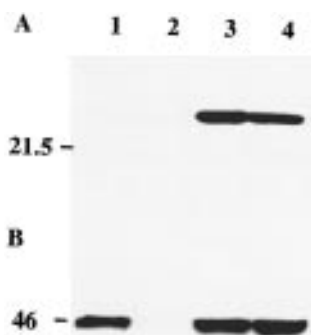


FIGURE 1: Reconstitution of yeast farnesyl-protein transferase activity from individual subunits expressed in bacteria. The FPTase activity present in bacterial extracts expressing Ram1 alone (lane 1) or Ram2 alone (lane 2) or after mixing extracts expressing Ram1 and Ram2 individually (lane 3) or together in the same bacterial strain (lane 4). Following electrophoresis, the bottom half of the gel was processed for fluorography to detect the [ $^3$ H]FPP-labeled 25-kDa Ras1T(CIIS) (A). The top half of the gel was used to perform an immunoblot to detect the presence of the 46-kDa myc-tagged Ram1 (B). The migration position and molecular masses of ovalbumin (46 kDa) and trypsin inhibitor (21.5 kDa) are indicated.

		83
Yeast Ram1 $\beta$	ALT----	KEFH
Hum FTase $\beta$	RLVLQREKHFH--	YLKRGRLR-QLT
Rat FTase $\beta$	RLVLQREKHFH--	YLDRLGLR-QLT
Yeast Cal1 $\beta$	RLVLQREKHFH--	YLKRGRLR-QLT
		156
Yeast Ram1 $\beta$	GGPFGGGPGQLS	HLASTYAAINALS
Hum FTase $\beta$	EGGFGGGPGQYP	HLAPTAAVNALC
Rat FTase $\beta$	DGGFGGGPGQYP	HLAPTAAVNALC
Yeast Cal1 $\beta$	HAT-----	TINLPNTLFALLSMI
		253 256 258
Yeast Ram1 $\beta$	GGFGSCPHVD	EAHGGYTFCATASLAIL
Hum FTase $\beta$	GGIGGVPGM-	EAHGGYTFCGLAALVIL
Rat FTase $\beta$	GGIGGVPGM-	EAHGGYTFCGLAALVIL
Yeast Cal1 $\beta$	GAFG----	HN-EPHGCMKF-----
		307 309
Yeast Ram1 $\beta$	RGFCGRSNKLV	DGCYSFWVGGSAAAIL
Hum FTase $\beta$	GGFQGRCNKLV	DGCYSFWQAGLLPLL
Rat FTase $\beta$	GGFQGRCNKLV	DGCYSFWQAGLLPLL
Yeast Cal1 $\beta$	GGFQGRGNKFA	DTCYAFWCLNSLHLL
		360 363 367
Yeast Ram1 $\beta$	GLRDKPGAHS	DFYHTNYCLLGLAVAE
Hum FTase $\beta$	GLLDKPGKSR	DFYHTCYCLSGLSIAQ
Rat FTase $\beta$	GLLDKPGKSR	DFYHTCYCLSGLSIAQ
Yeast Cal1 $\beta$	GFSKNDEEDAD	LYHSCLSGAALALIE

FIGURE 2: Amino acid sequence alignment of four conserved regions of the yeast (23), human (19), bovine, and rat (49) FPTase  $\beta$  subunits, as well as the yeast GGPTaseI  $\beta$  subunit (CALI) (13). Conserved His, Glu, and Asp residues mutated in this study are shaded (the numbering corresponds to the yeast Ram1 sequence).

to associate following affinity purification on nickel resin (Figure 3).

The effect of these mutations on FPTase activity was initially determined using a modified Ras1 protein, Ras1T(CIIS), and [ $^3$ H]FPP as substrates. A Ras1T(CIIS) concentration of 2  $\mu$ M was chosen to perform these assays after determining that the reaction rate was linear over a range from 0.2 to 2  $\mu$ M (data not shown). As seen in Figure 4 (panels A and C), four mutations (E256Q, D307N, C309A, and H363Q) cause a nearly complete loss of FPTase activity. Three of the mutant enzymes (H258N, D360N, and H156Q) have reduced but measurable FPTase activity. Glu256 and His258 are conserved in all prenyltransferases, whereas

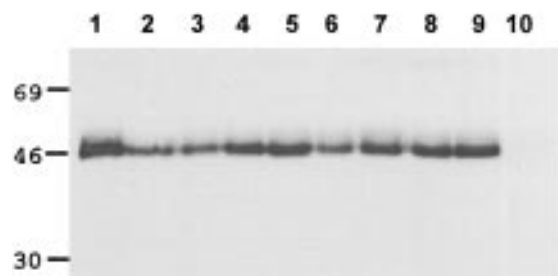


FIGURE 3: Posttranslational assembly of the Ram1/Ram2 heterodimer. Extracts from bacteria expressing myc-tagged Ram1 were mixed with lysates expressing (6xHis)-tagged Ram2, and the amount of complex formed was assessed following Ni-NTA affinity column chromatography. Complexes were analyzed by SDS-PAGE, and Ram1 was detected by immunoblot. Equivalent amounts of Ram2 extract were incubated with extracts expressing either wild-type Ram1 (lane 1), Ram1(H258N) (lane 2), Ram1(E256Q) (lane 3), Ram1(E256Q/H258N) (lane 4), Ram1(H253N) (lane 5), Ram1(H253N/H258N) (lane 6), Ram1(H363Q) (lane 7), Ram1(D360N) (lane 8), or Ram1(H156Q) (lane 9). Ram1 alone does not bind to the Ni-NTA affinity column under these conditions (lane 10). The molecular mass markers indicated on the left are bovine serum albumin (69 kDa), ovalbumin (46 kDa), and carbonyl anhydrase (30 kDa).

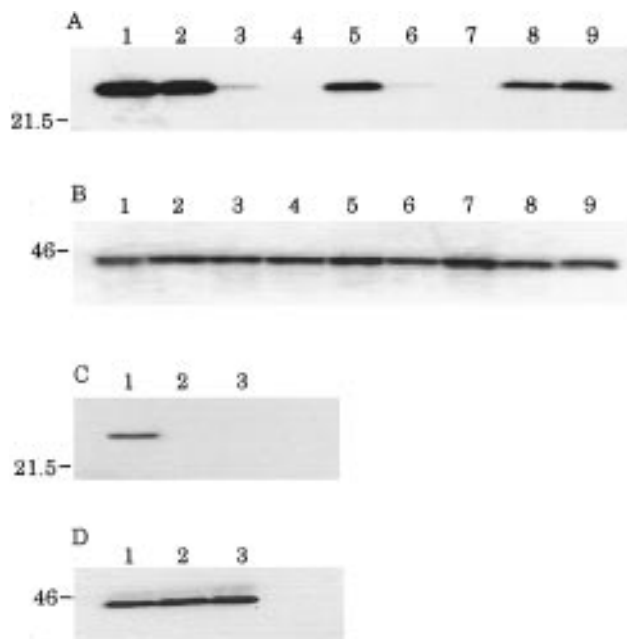


FIGURE 4: Relative FPTase activities of mutant Ram1 proteins. Panel A: [ $^3$ H]FPP-labeled Ras1T(CIIS) (25 kDa) product of the *in vitro* FPTase reaction visualized by fluorography. An equivalent amount of extract expressing Ram2 was mixed with wild-type Ram1 (lane 1), Ram1(H253N) (lane 2), Ram1(E256Q) (lane 3), Ram1(E256Q/H258N) (lane 4), Ram1(H258N) (lane 5), Ram1(H253N/H258N) (lane 6), Ram1(H363Q) (lane 7), Ram1(D360N) (lane 8), and Ram1(H156Q) (lane 9). Panel B: As described in the legend to Figure 1, the top half of the gel was transferred to nitrocellulose, and a Western blot was performed with monoclonal 9E10 to the myc-tagged Ram1 protein (46 kDa). The molecular mass markers indicated on the left are ovalbumin (46 kDa) and trypsin inhibitor (21.5 kDa).

His253 is found only in the yeast farnesyltransferase and geranylgeranyltransferase  $\beta$  subunits. Mutating His253 to Asn had no measurable effect on activity (Figure 4A, lane 2), but when it was mutated in combination with H258N FPTase activity was reduced to a level comparable to that of the E256Q mutant (Figure 4A, lane 6). The FPTase activity of the E256Q single and H253N/H258N double

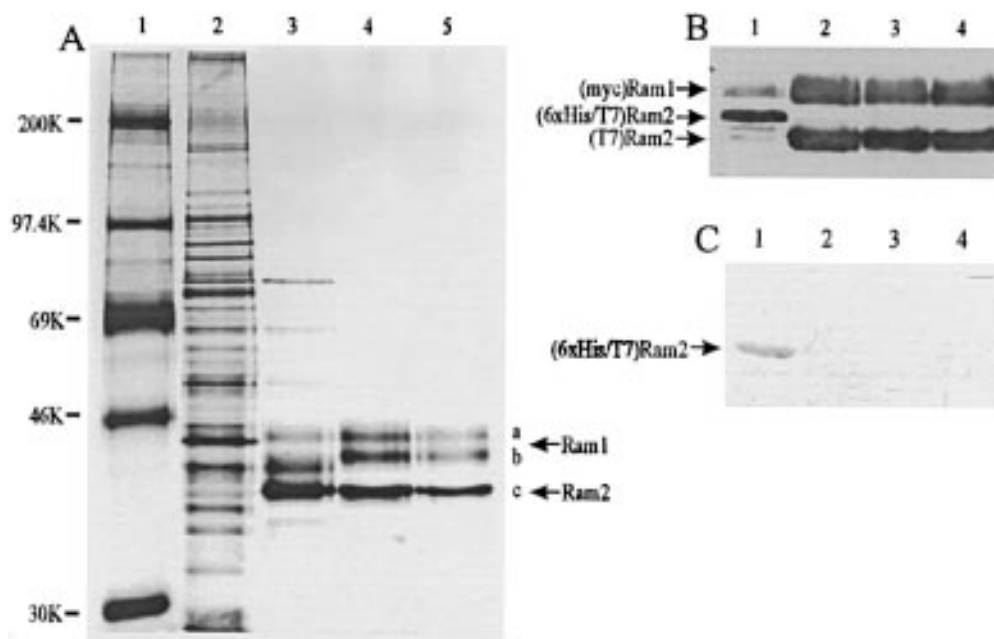


FIGURE 5: Purification of yeast FPTase. Panel A: Protein lysates from DE3 bacteria expressing wild-type FPTase before (lane 2) and after (lane 3) nickel affinity column purification were resolved by SDS-PAGE and visualized by silver staining. The nickel column-purified wild-type (lane 4) and similarly treated H258N mutant (lane 5) FPTase were further purified by chromatography on a MonoQ column. Molecular weight markers (lane 1) include myosin (200 kDa), phosphorylase b (97.4 kDa), bovine serum albumin (69 kDa), ovalbumin (46 kDa), and carbonic anhydrase (30 kDa). Note that the wild type and mutant Ram1 subunit appear as a doublet (a,b) due to proteolysis during the purification procedure. Panel B: Protein samples in panel A were loaded onto a separate 10% SDS-polyacrylamide gel, transferred to nitrocellulose, and blotted with monoclonal 9E10 (anti-myc) and anti-T7 epitope antibodies to the (myc)Ram1 and (6xHis/T7)Ram2 subunits. Samples include (1) cell-free extract, (2) wild type nickel column-purified, (3) wild-type FPTase after MonoQ purification, and (4) H258N FPTase after MonoQ purification. Panel C: Western blot probed with a Ni-NTA conjugate (Qiagen) to detect 6xHis epitope on Ram2. Lanes are as in panel B.

mutants was too low to perform detailed kinetic analysis so we turned our attention to the H258N mutant which appeared to be reduced by 50% when compared to wild-type FPTase.

**Catalytic Efficiency of Ram1(H258N) FPTase Is Reduced.** To investigate in more detail the defect caused by the H258N mutation, wild-type and mutant (H258N) FPTase enzymes were expressed as operon fusions in bacteria and purified by Ni affinity and ion-exchange (MonoQ) chromatography (Figure 5). Apparent  $K_m$  and  $V_m$  values were determined using a fluorescence FPTase assay (40, 41). Double-reciprocal plots of initial velocity data for wild-type and mutant FPTase are consistent with a sequential mechanism (Figure 6) (25–27). The apparent  $K_m$  values for the CaaX peptide and prenyl substrates increased 2–3-fold, and  $K_{cat}$  decreased 3.5-fold in the mutant Ram1(H258N)/Ram2 (Table 2). This corresponded to a 7–9-fold reduction in catalytic efficiencies ( $k_{cat}/K_{CIIS}$  and  $k_{cat}/K_{FPP}$ ). This agrees well with the qualitative gel assay of FPTase and indicates that one effect of mutating His258 may be to lower the binding affinity of both the CaaX and prenyl substrates.

**$Zn^{2+}$  Is Required for Farnesyl Pyrophosphate Binding to Yeast FPTase.** To determine if the decrease in catalytic efficiency observed in the mutants was due to a decrease in substrate binding, [ $^3H$ ]FPP binding was measured in the presence and absence of  $Zn^{2+}$ . In contrast to mammalian FPTase (33), FPP binding to the yeast enzyme requires  $Zn^{2+}$  (Figure 7). Therefore, the  $Zn^{2+}$  dependence of FPP binding provided a way in which to assess the Ram1 mutants. Reconstituted FPTase mutants were purified by nickel affinity chromatography, and [ $^3H$ ]FPP binding was measured. Ram1(H156Q), Ram1(H253N), and Ram1(D360N) mutants displayed FPP binding similar to wild-type enzyme. How-

ever, the binding of FPP to Ram1(H258N), Ram1(E256Q), Ram1(E256Q/H258N), Ram1(H253N/H258N), and Ram1-(H363Q) mutants was reduced by 70–94% compared to wild-type binding (background subtracted) (Table 3). Attempts to measure CaaX peptide binding or Ras1T(CIIS) cross-linking to yeast FPTase were unsuccessful (Farh, unpublished results).

**Measurement of the  $Zn^{2+}$  Dependence of FPTase Activity.** We investigated whether changing  $Zn^{2+}$  concentrations affects FPTase activity. This was done either by adding  $Zn^{2+}$  or by incubating with increasing concentrations of the  $Zn^{2+}$  chelator 1,10-phenanthroline. FPTase activity of wild-type and mutant Ram1(H258N) enzyme was compared following the addition of increasing amounts of 1,10-phenanthroline. As seen in Figure 8, the mutant enzyme was more sensitive to inhibition by 1,10-phenanthroline. The concentration required for 50% reduction in activity occurred at 0.5 and 0.2 mM 1,10-phenanthroline for the wild type and mutant, respectively (Figure 8, panels A and B). The mutant also required more  $Zn^{2+}$  to restore full activity to the apoenzyme. The concentration of  $Zn^{2+}$  required to restore 50% of the maximum FPTase activity to the wild type and mutant was 1.25 and 5  $\mu M$ , respectively (Figure 8, panels C and D). Taken together, it appears that the H258N FPTase mutant is more sensitive than the wild-type enzyme to  $Zn^{2+}$  concentrations.

**Mutations in Ram1 Cause Growth and Mating Defects when Expressed in Yeast.** Deletion of the *RAM1* gene in yeast results in a temperature-dependent growth defect and sterility due to a failure to process a-factor (19, 21). These phenotypes were used to assess the phenotypes of the Ram1 mutants *in vivo*. Yeast strains were constructed that

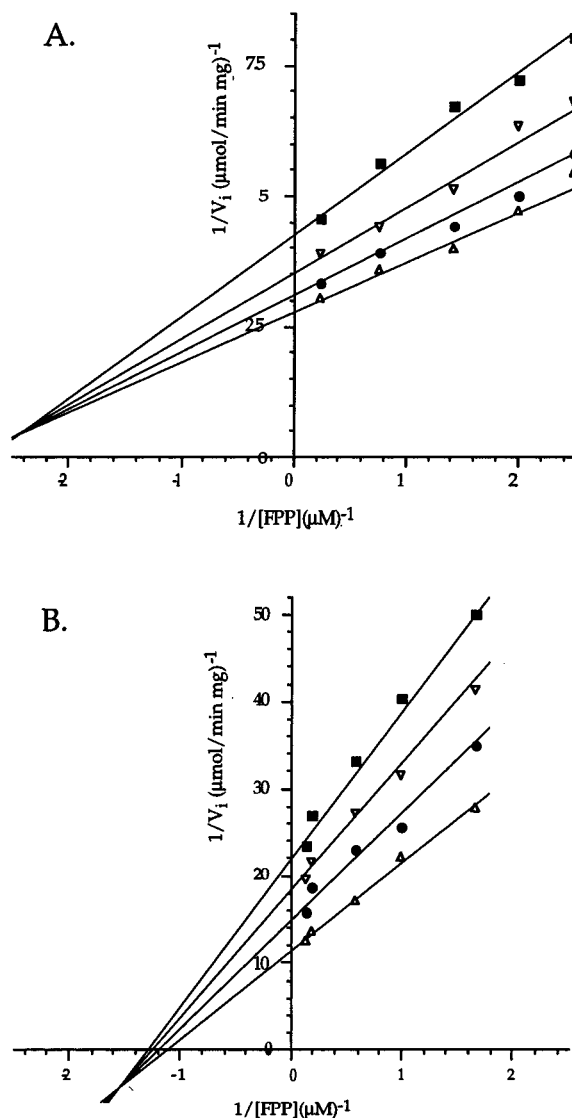


FIGURE 6: Initial velocity studies of (A) wild-type and (B) H258N mutant FPTases. Shown is the double-reciprocal plot of initial velocity vs varied concentrations of FPP ( $\mu\text{M}$ ) at different fixed concentrations of dansylated peptide (Dn-GCIIS). The concentrations of dansylated peptide used are  $0.5 \mu\text{M}$  ( $\blacksquare$ ),  $0.8 \mu\text{M}$  ( $\nabla$ ),  $1.2 \mu\text{M}$  ( $\bullet$ ), and  $2.0 \mu\text{M}$  ( $\Delta$ ) for wild-type FPTase and  $0.6 \mu\text{M}$  ( $\blacksquare$ ),  $0.8 \mu\text{M}$  ( $\nabla$ ),  $1.2 \mu\text{M}$  ( $\bullet$ ), and  $2.4 \mu\text{M}$  ( $\Delta$ ) for the H258N FPTase mutant. Each point is the average of at least three trials.

Table 2: FPTase Kinetic Activity Comparison<sup>a</sup>

		wild type	H258N
$K_{\text{CIIS}}$	( $\mu\text{M}$ )	$0.43 \pm 0.06$	$1.1 \pm 0.2$
$K_{\text{FPP}}$	( $\mu\text{M}$ )	$0.33 \pm 0.05$	$1.0 \pm 0.2$
$V_{\text{max}}$	( $\mu\text{mol}/\text{min} \cdot \text{mg}$ )	$0.44 \pm 0.02$	$0.13 \pm 0.01$
$k_{\text{cat}}$	( $\text{s}^{-1}$ )	$0.63 \pm 0.04$	$0.18 \pm 0.01$
$k_{\text{cat}}/K_{\text{CIIS}}$	( $\text{M}^{-1} \text{s}^{-1} \times 10^5$ )	$15 \pm 2$	$1.7 \pm 0.3$
$k_{\text{cat}}/K_{\text{FPP}}$	( $\text{M}^{-1} \text{s}^{-1} \times 10^5$ )	$19 \pm 3$	$1.8 \pm 0.4$

<sup>a</sup> Kinetic parameters were determined as described in Experimental Procedures from the initial velocity data plotted in Figure 6. Initial velocities in  $\Delta F$  (s) were converted to  $\mu\text{mol}/\text{min} \cdot \text{mg}$  as described in ref 41 using protein concentrations determined by the Bradford assay.

expressed wild-type *RAM1* or one of the four *RAM1* mutants: Ram1(H258N), Ram1(E256Q), Ram1(E256Q/H258N), and Ram1(H253N/H258N). The wild-type strain had a doubling time of 1.9 h, whereas the mutants grew more slowly with doubling times of 2.1 h (H258N), 3.8 h (E256Q), and 2.8 h (H253N/H258N) (Table 4). Using sensitive mating

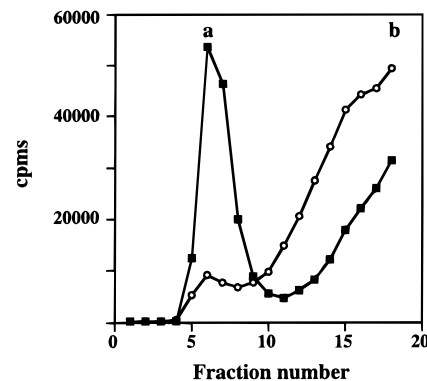


FIGURE 7:  $\text{Zn}^{2+}$  requirement for  $[^3\text{H}]$ FPP binding to yeast FPTase. Ram1/Ram2 protein was purified by Ni affinity column chromatography, and FPP binding assays were conducted as described in Experimental Procedures. The Ram1/Ram2 complex was extensively dialyzed in EDTA-containing buffer and then incubated with  $[^3\text{H}]$ FPP in buffer containing  $5 \text{ mM}$   $\text{MgCl}_2$  and  $20 \mu\text{M}$   $\text{ZnCl}_2$  ( $\blacksquare$ ), or  $5 \text{ mM}$   $\text{MgCl}_2$  alone ( $\circ$ ). The elution position of bound (a) and free (b)  $[^3\text{H}]$ FPP is indicated. Similar results were obtained in three independent experiments.

Table 3:  $[^3\text{H}]$ Farnesyl Pyrophosphate Binding to Reconstituted Yeast FPTase

FPTase <sup>a</sup>		bound FPP (pmol) <sup>b</sup>
$\alpha$	$\beta$	
none	none	1.04
Ram2	none	$0.98 \pm 0.03$
Ram2	Ram1	$5.50 \pm 0.38$
Ram2	Ram1(H156Q)	$4.92 \pm 0.27$
Ram2	Ram1(H253N)	$6.96 \pm 0.88$
Ram2	Ram1(H258N)	$2.36 \pm 0.35$
Ram2	Ram1(H253N/H258N)	$1.45 \pm 0.14$
Ram2	Ram1(E256Q)	$1.92 \pm 0.25$
Ram2	Ram1(E256Q/H258N)	$1.27 \pm 0.01$
Ram2	Ram1(D360N)	$5.86 \pm 0.24$
Ram2	Ram1(H363Q)	$1.76 \pm 0.05$

<sup>a</sup> Ram1 and Ram2 were expressed in bacteria, extracts were mixed, and reconstituted FPTase was purified using Ni affinity chromatography. Enzyme was eluted with imidazole and FPP binding measured by a gel filtration. The assay is described in detail in Experimental Procedures. <sup>b</sup> Average of two independent experiments.

assays, we found that Ram1(E256Q)- or Ram1(E256Q/H258N)-expressing strains were sterile with mating frequencies similar to a *ram1* deletion strain. Partial mating was observed with the less severe Ram1 mutants (Table 4).

## DISCUSSION

Site-directed mutagenesis of the yeast FPTase  $\beta$  subunit was performed in an attempt to better understand the role of  $\text{Zn}^{2+}$  in catalysis. Four mutants, E256Q, D307N, C309A, and H363Q, had the most severe reduction in FPTase activity both *in vitro* and *in vivo*. D307N, C309A, and His363 correspond to residues in the mammalian enzyme that, along with a water molecule, directly ligand  $\text{Zn}^{2+}$  in the mammalian FPTase crystal structure (33).  $\text{Zn}^{2+}$  is believed to play a direct role in catalysis by coordinating the thiol of the CaaX substrate in the enzyme-FPP-peptide substrate ternary complex (45, 32). As expected, mutating His363 to Asn abolishes  $^{65}\text{Zn}^{2+}$  binding (data not shown). In addition to His363, we also mutated Asp360 and Cys367, two other conserved residues in the vicinity of the  $\text{Zn}^{2+}$  ligand His363. Cys367 is conserved among all farnesyl-protein transferases but not geranylgeranyl-protein transferases. The Cys residue

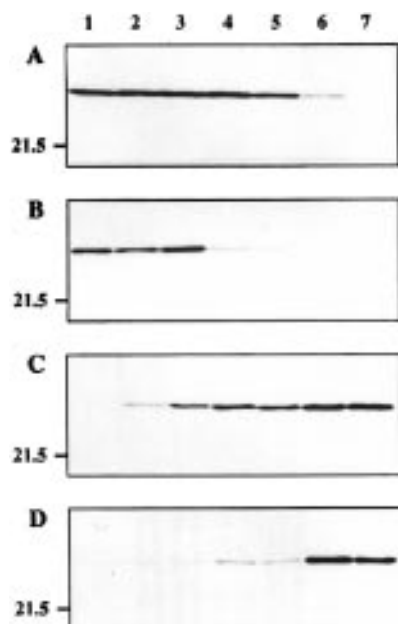


FIGURE 8: Comparison of the  $\text{Zn}^{2+}$  binding properties of the FPTases composed of wild-type Ram1 or mutant Ram1(H258N). The relative  $\text{Zn}^{2+}$  affinity of the wild-type Ram1 (A) or Ram1(H258N) mutant (B) enzyme was assessed by its sensitivity to 1,10-phenanthroline. The concentration of 1,10-phenanthroline added was no addition (lane 1), 0.0625 mM (lane 2), 0.125 mM (lane 3), 0.25 mM (lane 4), 0.5 mM (lane 5), 1 mM (lane 6), and 2 mM (lane 7). The concentrations of  $\text{Zn}^{2+}$  required to restore FPTase activity to the enzyme following removal of  $\text{Zn}^{2+}$  with EDTA was also measured (C and D). The FPTase activities of equivalent amounts of wild-type (C) or mutant Ram1(H258N) (D)  $\text{Zn}^{2+}$ -free apoenzyme were measured when 0.625  $\mu\text{M}$  (lane 2), 1.25  $\mu\text{M}$  (lane 3), 2.5  $\mu\text{M}$  (lane 4), 5  $\mu\text{M}$  (lane 5), 10  $\mu\text{M}$  (lane 6), and 20  $\mu\text{M}$  (lane 7)  $\text{ZnCl}_2$  were present in the reactions. The products of the reactions were analyzed by SDS-PAGE followed by fluorography. The exposure time for films of the wild-type Ram1 enzyme (A and C) was 12 h and for the Ram1(H258N) enzyme (B and D) 30 h. Similar results were obtained in three independent experiments.

Table 4: Doubling Time and Mating Efficiency of RJY871 Expressing Ram1 Mutants

plasmid	doubling time (h) <sup>a,b</sup>	relative mating efficiency <sup>a,c</sup>
pSB32Ram1	1.9	1
pSB32Ram1(H258N)	2.1	0.61
pSB32Ram1(E256Q)	3.8	$<1.4 \times 10^{-8}$
pSB32Ram1(E256Q/H258N)	3.5	$<1.7 \times 10^{-8}$
pSB32Ram1(H253N/H258N)	2.8	0.04
pSB32	3.7	$<2.0 \times 10^{-8}$

<sup>a</sup> Average of two experiments. <sup>b</sup> Experiments performed at 30 °C. <sup>c</sup> Experiments performed at 24 °C.

corresponding to Cys367 in mammalian FPTase reacts with *N*-ethylmaleimide (NEM), but only after  $\text{Zn}^{2+}$  is removed with EDTA suggesting that this Cys might also play a role coordinating  $\text{Zn}^{2+}$  (45). However, mutating Cys367 to Ala had little effect on FPTase activity. Similarly, mutating Asp360 to Asn had only a minimal effect on activity. The reason for a decrease in FPTase activity in the E256Q mutant is less clear. In the mammalian crystal structure, Glu256 is located in a loop connecting helices 8 $\beta$  and 9 $\beta$  in the region of the  $\beta$  subunit forming the entrance to the FPP binding cleft (33). We find that FPP binding is significantly reduced in the E256Q mutant FPTase, but it seems unlikely that the carboxyl group of Glu directly contributes to FPP binding. Glu256 is also located close to the  $\alpha/\beta$ -subunit interface

raising the possibility that an important  $\alpha$ - $\beta$  interaction occurs through this region. Although the  $\beta$  subunit is primarily responsible for CaaX and FPP substrate binding, the  $\alpha$  subunit also influences substrate recognition (46). Mutating Glu256 has no measurable effect on the ability of Ram1 to bind to Ram2 during purification but could affect substrate binding through more localized interactions.

The H258N mutant exhibited lower but measurable FPTase activity allowing the kinetic properties to be investigated using a sensitive fluorescence assay. Mutating His258 to Asn increased the  $K_m$  for both substrates 2–3-fold and decreased the  $K_{cat}$  3.5-fold. Overall, this leads to a 7–9-fold decrease in catalytic efficiency. His258 corresponds to His248 in the mammalian enzyme which is seen in the crystal structure to make a hydrogen bond with a nonapeptide from an adjacent  $\beta$  subunit in the crystal lattice (33). It has been suggested that this is the peptide substrate binding site, but it is appropriate to view this with caution. First, the nonapeptide lacks the Cys of the CaaX box which is a major determinant of substrate recognition. Second, there is no FPP bound to the enzyme in this structure. FPP binds to the enzyme first and affects the affinity of the peptide substrate (25). Furthermore, FPP binding is accompanied by a conformational change in the enzyme, although the effect of this conformational change on peptide substrate binding has not been characterized (47). Further work is needed to define the residues important for substrate binding and to determine the role of the  $\text{Zn}^{2+}$  in catalysis. Interestingly, the activity of the H258N mutant could be restored to close to wild-type levels by elevating the concentration of  $\text{Zn}^{2+}$ .

Two of the original Ram1 mutants identified by yeast genetic screens, *ram1-1* and *ram1-2*, result in the changes D209N and G259V, respectively. These mutations fall in highly conserved regions between members of the prenyl-transferase family and in the case of G259 mutate a residue very close to the E256Q and H258N mutations we have shown affect yeast FPTase activity. Omer et al. (48) have studied the kinetic properties of the human FPTase harboring mutations corresponding to the yeast *Ram1-1* and *Ram1-2* alleles. The G259V mutation affects the  $K_m$  for FPP, increasing it 10–100-fold depending on the –aaX sequence of the CaaX protein substrate used. Likewise, the  $K_m$  for the CaaX substrate increases by approximately 5-fold compared to wild-type enzyme. This is very similar to the H258N mutation suggesting an important role for this region in controlling substrate access to the active site.

Although the properties of the yeast and mammalian FPTases are very similar, notable differences exist. The  $\alpha$  subunit (Ram1) of yeast is smaller than its mammalian counterpart (316 aa vs 377 aa) and lacks the stretch of nine prolines at the amino terminus that causes the aberrant migration of the mammalian enzyme SDS-PAGE. The  $\beta$  subunits are much more similar, but again significant differences are observed. FPP binding is  $\text{Zn}^{2+}$ -dependent in the case of the yeast enzyme, whereas FPP binding to mammalian FPTase is  $\text{Zn}^{2+}$ -independent (31). The affinity of the enzyme for FPP is also different. The  $K_{FPP}$  for mammalian FPTase is 10 nM, whereas  $K_{FPP}$  of the yeast enzyme is 330 nM. Although the reasons for these differences are not known, the decrease in FPTase activity of the Ram1 mutants we describe here correlates well with their ability to bind FPP (Table 3). Since FPP binds FPTase first

and influences the binding of the CaaX substrate, the decrease in FPP binding observed in the H258N, E256Q, and H363Q mutants also decreases the affinity of the CaaX substrate resulting in the overall reduction in FPTase activity that is observed.

Yeast provides a powerful system in which to study protein prenylation. Deletion of *RAM1* results in a temperature-sensitive growth defect and sterility if the mutation occurs in a *MATa* haploid yeast strain (8, 16, 17). Both phenotypes are easily exploited to evaluate the activity of *RAM1* mutants. Quantitative mating assays are particularly useful because mating efficiencies can be measured over a range of 7 orders of magnitude. In this study, the results of mating assays were in close agreement with FPTase enzyme assays performed on recombinant proteins purified from bacteria. The bacterial and yeast expression systems described here provide rapid and convenient methods for measuring expression, dimer assembly, and FPTase activity of wild-type and mutant FPTase subunits.

## ACKNOWLEDGMENT

We thank Scott Powers (Onyx Pharmaceuticals), Dr. Susan Michaelis (Johns Hopkins University), and Dr. Mark Marshall for providing plasmids and yeast strains. We especially appreciate the generous gift of purified Ras1T(CIIS) provided by Dr. Mark Marshall. The helpful comments of Bryce Plapp, Peter Rubenstein, Dan Weeks, and members of the laboratory are very appreciated.

## REFERENCES

- Deschenes, R. J., Resh, M. D., & Broach, J. R. (1990) *Curr. Opin. Cell Biol.* 2, 1108–1113.
- Schafer, W. R., & Rine, J. (1992) *Annu. Rev. Genet.* 26, 209–237.
- Clarke, S. (1992) *Annu. Rev. Biochem.* 61, 355–386.
- Zhang, F. L., & Casey, P. J. (1996) *Annu. Rev. Biochem.* 65, 241–269.
- Hancock, J. F., Magee, A. I., Childs, J. E., & Marshall, C. J. (1989) *CELL* 57, 1167–1177.
- Reiss, Y., Goldstein, J. L., Seabra, M. C., Casey, P. J., & Brown, M. S. (1990) *CELL* 62, 81–88.
- Moores, S. L., Schaber, M. D., Mosser, S. D., Rands, E., O'Hara, M. B., Garsky, V. M., Marshall, M. S., Pompliano, D. L., & Gibbs, J. B. (1991) *J. Biol. Chem.* 266, 14603–14610.
- He, B., Chen, P., Chen, S.-Y., Vancura, K. L., Michealis, S., & Powers, S. (1991) *Proc. Natl. Acad. Sci. U.S.A.* 88, 11373–11377.
- Kawata, M., Farnsworth, C. C., Yoshida, Y., Gelb, M. H., Glomset, J. A., & Takai, Y. (1990) *Proc. Natl. Acad. Sci. U.S.A.* 87, 8960–8964.
- Ohya, Y., Goebel, M., Goodman, L. E., Petersen-Bjorn, S., Friesen, J. D., Tamanoi, F., & Anraku, Y. (1991) *J. Biol. Chem.* 266, 12356–12360.
- Mayer, M. P., Prestwich, G. D., Dolence, J. M., Bond, P. D., Wu, H., & Poulter, C. D. (1993) *Gene* 132, 41–47.
- Trueblood, C. E., Ohya, Y., & Rine, J. (1993) *Mol. Cell. Biol.* 13, 4260–4275.
- Caplin, B. E., Hettich, L. A., & Marshall, M. S. (1994) *Biochim. Biophys. Acta* 1205, 39–48.
- Horiuchi, H., Kawata, M., Katayama, M., Yoshida, Y., Musha, T., Ando, S., & Takai, Y. (1991) *J. Biol. Chem.* 266, 16981–16984.
- Seabra, M. C., Goldstein, J. L., Südhof, T. C., & Brown, M. S. (1992) *J. Biol. Chem.* 267, 14497–14503.
- Powers, S., Michaelis, S., Broek, D., Santa Anna, S., Field, J., Herskowitz, I., & Wigler, M. (1986) *CELL* 47, 413–422.
- Fujiyama, A., Matsumoto, K., & Tamanoi, F. (1987) *EMBO J.* 6, 223–228.
- Goodman, L. E., Perou, C. M., Fujiyama, A., & Tamanoi, F. (1988) *Yeast* 4, 271–281.
- Kohl, N. E., Diehl, R. E., Schaber, M. D., Rands, E., Soderman, D. D., He, B., Moores, S. L., Pompliano, D. L., Ferro-Novick, S., Powers, S., Thomas, K. A., & Gibbs, J. B. (1991) *J. Biol. Chem.* 266, 18884–18888.
- Schafer, W. R., Trueblood, C. E., Yang, C.-C., Mayer, M. P., Rosenberg, S., Poulter, C. D., Kim, S.-H., & Rine, J. (1990) *Science* 249, 1133–1139.
- Goodman, L. E., Judd, S. R., Farnsworth, C. C., Powers, S., Gelb, M. H., Glomset, J. A., & Tamanoi, F. (1990) *Proc. Natl. Acad. Sci. U.S.A.* 87, 9665–9669.
- Mayer, M. L., Caplin, B. E., & Marshall, M. S. (1992) *J. Biol. Chem.* 267, 20589–20593.
- Seabra, M. C., Reiss, Y., Casey, P. J., Brown, M. S., & Goldstein, J. L. (1991) *CELL* 65, 429–434.
- Pompliano, D. L., Rands, E., Schaber, M. D., Mosser, S. D., Anthony, N. J., & Gibbs, J. B. (1992b) *Biochemistry* 31, 3800–3807.
- Pompliano, D. L., Schaber, M. D., Mosser, S. D., Omer, C. A., Shafer, J. A., & Gibbs, J. B. (1993) *Biochemistry* 32, 8341–8347.
- Gomez, R., Goodman, L. E., Tripathy, S. K., O'Rourke, E., Manne, V., & Tamanoi, F. (1993) *Biochem. J.* 289, 25–31.
- Dolence, J. M., & Poulter, C. D. (1995) *Proc. Natl. Acad. Sci. U.S.A.* 92, 5008–5011.
- Furfine, E. S., Leban, J. J., Landovazo, A., Moomaw, J. F., & Casey, P. J. (1995) *Biochemistry* 34, 6857–6862.
- Tschantz, W. R., Furfine, E. S., & Casey, P. J. (1997) *J. Biol. Chem.* 272, 9989–9993.
- Reiss, Y., Seabra, M. C., Armstrong, S. A., Slaughter, C. A., Goldstein, J. L., & Brown, M. S. (1991) *J. Biol. Chem.* 266, 10672–10677.
- Reiss, Y., Brown, M. S., & Goldstein, J. L. (1992) *J. Biol. Chem.* 267, 6403–6408.
- Huang, C. C., Casey, P. J., & Fierke, C. A. (1997) *J. Biol. Chem.* 272, 20–23.
- Park, H.-W., Boduluri, S. R., Moomaw, J. F., Casey, P. J., & Beese, L. S. (1997) *Science* 275, 1800–1804.
- Sherman, F., Fink, G. R., & Hicks, J. B. (1986) *Laboratory Course Manual: Methods in Yeast Genetics*, Cold Spring Harbor Laboratory, Cold Spring Harbor, NY.
- Caplin, B. E., & Marshall, M. S. (1995) *Methods Enzymol.* 250, 51–68.
- Rose, M. D., Novick, P., Thomas, J. H., Botstein, D., & Fink, G. R. (1987) *Gene* 60, 237–243.
- Mitchell, D. A., Marshall, T. K., & Deschenes, R. J. (1993) *Yeast* 9, 715–723.
- Ito, H., Fukada, Y., Murata, K., & Kimura, A. (1983) *J. Bacteriol.* 153, 163–168.
- Robzyk, K., & Kassir, Y. (1992) *Nucleic Acids Res.* 20, 3790.
- Pompliano, D. L., Gomez, R. P., & Anthony, N. J. (1992a) *J. Am. Chem. Soc.* 114, 7945–7946.
- Bond, P. D., Dolence, J. M., & Poulter, C. D. (1995) *Methods Enzymol.* 250, 30–43.
- Orr-Weaver, T. L., Szostak, J. W., & Rothstein, R. J. (1983) *Methods Enzymol.* 101, 228–245.
- Chen, W.-J., Andres, D. A., Goldstein, J. L., Russell, D. W., & Brown, M. S. (1991) *CELL* 66, 327–334.
- Andres, D. A., Goldstein, J. L., Ho, Y. K., & Brown, M. S. (1993) *J. Biol. Chem.* 268, 1383–1390.
- Fu, H. W., Moomaw, J. F., Moomaw, C. R., & Casey, P. J. (1996) *J. Biol. Chem.* 271, 28541–28548.
- Pellicena, P., Scholten, J. D., Zimmerman, K., Creswell, M., Huang, C. C., & Miller, W. T. (1996) *Biochemistry* 35, 13494–13500.
- Wallace, A., Koblan, K. S., Hamilton, K., Marquis-Omer, D. J., Miller, P. J., Mosser, S. D., Omer, C. A., Schaber, M. D., Cortese, R., Oliff, A., Gibbs, J. B., & Pessi, A. (1996) *J. Biol. Chem.* 271, 31306–31311.
- Omer, C. A., Kral, A. M., Diehl, R. E., Prendergast, G. C., Powers, S., Allen, C. M., Gibbs, J. B., & Kohl, N. E. (1993) *Biochemistry* 32, 5167–5176.